Efficient Valuation of Equity-Indexed Annuities Under Lévy Processes Using Fourier-Cosine Series

Geng Deng, PhD, CFA, FRM[*] Tim Dulaney, PhD, FRM[†,‡]
Craig McCann, PhD, CFA[§] Mike Yan, PhD, FRM[¶]

April 1, 2014

Abstract

Equity-Indexed Annuities (EIAs) are deferred annuities which accumulate value over time according to crediting formulas and realized equity index returns. We propose an efficient algorithm to value two popular crediting formulas found in EIAs – Annual Point-to-Point (APP) and Monthly Point-to-Point (MPP) – under general Lévy-process based index returns. APP contracts observe returns of referenced indexes annually and credit EIA accounts, subject to minimum and maximum returns. MPP contracts incorporate both local/monthly caps and global/annual floors on index credits. MPP contracts have payoffs of a "cliquet" option.

Our algorithm, based on the COS method (Fang and Oosterlee, 2008), expands the present value of an EIA contract using Fourier-cosine series, and expresses the value of the EIA contract as a series of terms involving simple characteristic function evaluations. We present several examples with different Lévy processes, including the Black-Scholes model and the CGMY model. These examples illustrate the efficiency of our algorithm as well as its versatility in computing annuity market sensitivities, which could facilitate the hedging and pricing of annuity contracts.

1 Introduction

Equity-Indexed Annuities (EIAs) are deferred annuities which credit interest to the account and determine other benefits associated with the annuity according to the evolution of one or more

[*]Director of Research, Office: (703) 890-0741 or Email: GengDeng@slcg.com

[†]Financial Analyst, U.S. Securities and Exchange Commission dulanyt@sec.gov

[‡]The Securities and Exchange Commission, as a matter of policy, disclaims responsibility for any private publication or statement by any of its employees. The views expressed herein are those of the author and do not necessarily reflect the views of the Commission or of the author's colleagues upon the staff of the Commission.

[§]President, Office: (703) 539-6760 or Email: CraigMcCann@slcg.com.

[¶]Senior Financial Economist, Office: 703-539-6780 or Email: MikeYan@slcg.com

underlying equity indexes operating through a crediting formula.

EIAs specify a minimum rate of return and the potential for further gains depending on the linked index or indexes. EIAs accumulate credits in an account value during a "deferral period" and then after the end of the deferral period the account value can be cashed out or annuitized during the "annuitization period".

Rather than simple direct exposure to stock market returns, EIAs generally use complex crediting formulas to determine annual credits and, eventually, the amount that is available to be annuitized. The common point-to-point crediting formula can be further differentiated by the frequency that the returns are observed:

- *Annual Point-to-Point (APP)* contracts observe percentage changes in the linked index level or levels annually and credit investors' account values subject to an annual floor and cap. If the index return is below a guaranteed minimum rate, this minimum rate is credited.

- *Monthly Point-to-Point (MPP)* contracts observe percentage changes in the index levels monthly. On each policy anniversary, the monthly capped index returns for the twelve preceding months are summed to produce the annual crediting rate. The greater of this rate and the guaranteed minimum rate specified by the contract is then applied to the account value.

APP contracts have the payoff of plain vanilla European options annually. MPP contract payoffs are path-dependent within each contract year. In this paper, we advocate a unified valuation approach for both APP and MPP type contracts.

EIA crediting formulas have been studied previously in literature. Tiong (2010) values several EIA types, including point-to-point, using Esscher transforms and assuming geometric Brownian motion. Lee (2003) constructs and values alternative EIAs with barrier options. Lin and Tan (2003) provide pricing formulas for several types of EIAs using an asset price that follows geometric Brownian motion with stochastic interest rates. Jaimungal (2004) develops closed-form expressions for the prices of point-to-point EIAs assuming the underlying asset follows a – Variance Gamma (VG) process.[1] Jaimungal and Young (2005) explore the effect of heavy-tailed asset returns on the valuation of EIAs. Gaillardetz and Lin (2006) study the effect on the valuation of EIAs of dropping the usual assumption that mortality risk can be diversified. Boyle and Tian (2008) apply constraints based on investor preferences to provide optimal EIA contract designs from the investor's prospective. Kijima and Wong (2007) include the effect of stochastic interest rates using an extended Vasicek model for the valuation of ratchet EIAs. Yuen and Yang (2010) find that a trinomial tree method can be efficient when valuing EIA's with embedded Asian options using a regime-switching model with stochastic interest rates and volatility.

MPP contracts specify a minimum return at contract anniversaries while applying local caps to each monthly return. Cliquet options, cited by Wilmott (2002) as "the height of fashion in

[1] There is some discrepancy between the European call option valuation formula in the literature. See Madan et al. (1998), Jaimungal (2004), and Ballotta (2010) for three examples.

the world of equity derivatives," are solved using an adaptive partial differential equation method within a constant volatility environment. Windcliff et al. (2006) describe several numerical issues that arise when valuing cliquet options. More recently, Madan and Shoutens (2013) study the dynamics of market prices for a sample of cliquet options and find that call options can be used as effective hedges in certain cases.

Bernard et al. (2011) show that the marketing materials for EIAs embedding cliquet options present overly optimistic scenarios, that the products tend to underperform in turbulent markets, and that the specific EIAs studied were overpriced by approximately 6.5%. Bernard and Boyle (2011) illustrate that insurers can reduce their exposure to volatile market conditions by diversifying their offering of EIAs.

Our contribution to the growing EIA literature is our implementation of an option pricing methodology that is applicable generally to any (exponential) Lévy model of asset returns with a closed-form characteristic function. The generality of this methodology allows researchers and practitioners to isolate the effects of model peculiarities and more efficiently compute numerical valuations and market sensitivities (Greeks).

The COS method valuation methodology – a numerical approximation based upon the Fourier-cosine series expansion – was developed by Fang and Oosterlee (2008). Fang and Oosterlee (2008) show that the convergence rate for this method is exponential with linear computational complexity in most cases. The method was then used to price early-exercise and discrete barrier options in Fang and Oosterlee (2009), Asian options in Zhang and Oosterlee (2013), and Bermudan options in the Heston model in Fang and Oosterlee (2011). Our paper applies this Fourier-cosine series methodology to the valuation of APP and MPP annuities.

We apply two levels of the COS method in our valuations. The first application expands the annuity value as a series of terms based on valuations of the characteristic function of 'global capped returns.' An advantage of the COS method, or of the separation feature in the method, is that all information about the return distribution is derived from the characteristic function; while the structural information of the EIA contract, such as caps and floors, are contained in the Fourier coefficients. Our methodology facilitates the application of various characteristic functions to value the EIA contract efficiently.

The second application of the COS method is to construct the characteristic function of the capped local returns, which is also expanded as a series of terms based on the characteristic function of the uncapped local returns. As in the first level application of the COS method, information about the local cap is contained in the coefficients of the series. The methodology simplifies the computation of Greeks for EIA contracts and, therefore, helps issuers more easily understand and hedge their liabilities.

The approach advocated here is generally applicable and efficient for EIAs and EIA Greeks valuation in any Lévy based model. We provide examples of various Lévy models, including the Black-Scholes model and the CGMY model of which the Variance Gamma (VG) model is a special case.

Our paper is arranged as follows. Section 2 specifies the APP and MPP crediting formulas. Section 3 introduces the COS method and develops a two-level application to be used to value the EIA contract. Section 4 introduces an alternative approach, values Greeks and implements several Lévy process models. Section 5 provides numerical results and an analysis of the efficiency of our proposed algorithm.

2 Point-to-Point Equity-Indexed Annuities

On contract anniversaries, EIAs credit the account value of the contract holder with payments based on predetermined crediting formulas.[2] APP specifies an annual cap (c) and floor (g) that are applied to the index returns. Let $S(t)$ be levels of the underlying index and K be the initial annuity account value at $t = 0$. At the end of one year ($T = 1$), the accumulated account value is

$$v_{APP}(D) = K \max(1 + g, 1 + D) = K \max\left(1 + g, 1 + \min(c, R_T)\right). \tag{1}$$

where R_T is the annual index return, defined as

$$R_T = \frac{S(T) - S(0)}{S(0)}. \tag{2}$$

Here the guaranteed minimum return (g) acts as a floor for the time period. The new return variable

$$D = \min(c, R_T),$$

represents a capped annual return. In the analysis that follows, we will directly model the characteristic function of the return variable D.

The second crediting formula, MPP, calculates annual account credits based on the monthly returns of the underlying index. First, let us define the monthly observation dates $t_0 = 0, t_1, \ldots, t_{12} = 1$ satisfying $t_j - t_{j-1} = \Delta = \frac{1}{12}$, for $j = 1, \ldots, 12$. The monthly index returns R_j are thus defined as

$$R_j = \frac{S(t_j) - S(t_{j-1})}{S(t_{j-1})}, \text{ for } j = 1, \ldots, 12. \tag{3}$$

At the end of one year, the accumulated account value is

$$v_{MPP}(D) = K \max(1 + g, 1 + D) = K \max\left(1 + g, 1 + \sum_{j=1}^{12} \min(c, R_j)\right), \tag{4}$$

where c is a monthly return cap (not annualized). For MPP contracts, the cap is sometimes referred to as a "local cap" since the monthly returns are capped prior to applying the guaranteed

[2] Almost all EIA contracts include an annual reset feature. This feature guarantees that each non-negative annual return is locked in.

minimum return – sometimes referred to as the "global floor." Here the capped return variable becomes

$$D = \sum_{j=1}^{12} \min(c, R_j).$$

Note that the range of the variable D is $(-12, 12c]$, since R_j is bounded below by -1.

The present value of the annuity contract at time $t = 0$ (under the risk neutral measure $\mathbb{Q}$) is discounted expected payoff

$$PV_{APP} = e^{-\hat{r}T}\mathbb{E}^{\mathbb{Q}}\left[v_{APP}(D)\right] = e^{-\hat{r}T}\int_{-\infty}^{\infty} v_{APP}(y)f_D(y)dy, \tag{5}$$

and similarly, for MPP

$$PV_{MPP} = e^{-\hat{r}T}\mathbb{E}^{\mathbb{Q}}\left[v_{MPP}(D)\right], \tag{6}$$

where $\hat{r}$ is an insurer rate reflecting the credit risk of the issuer in light of any state guarantees, and $f_D(y)$ is the probability density function (PDF) of the return variable D under the risk-neutral measure $\mathbb{Q}$.

To present a unified approach to both "APP" and "MPP," we introduce n as the number of observation periods. The capped return D is rewritten as

$$D = \sum_{j=1}^{n} \min(c, R_j). \tag{7}$$

APP uses a single annual observation period ($n = 1$) and MPP uses monthly observation periods ($n = 12$). In the following section, we will drop the subscripts "APP"and "MPP" for convenience.

3 Valuation Methodology

3.1 Introduction to the COS method

The key idea behind the COS method is to project the integral involving a density function – see Equation (5) – of a random variable onto the space spanned by a Fourier-cosine basis $\{\cos(\frac{k\pi(y-a)}{b-a})|k = 0, 1, 2, 3, \ldots\}$. This relies on the fact that the density function as well as the component payoff function in the integral form can both be spanned by the Fourier-cosine basis, on a truncated range $[a, b]$. More details of the method and its convergence analysis can be found in Fang and Oosterlee (2008).

The expected payoff of a financial instrument, before any discount, is generally given by the integral form

$$P = \int_{\mathbb{R}} v(y)f(y)dy. \tag{8}$$

Where $v(y)$ is a payoff function determined by the structure of the financial instrument. The COS method applies three approximations to this payoff calculation.

1. *Compactly Supported Approximation*: The first step is to truncate the integral region from $\mathbb{R}$ to $[a,b]$ then

$$P_1 = \int_a^b v(y)f(y)dy. \tag{9}$$

In order to minimize the truncation errors, we choose the a and b such that the density function $f(y)$ concentrates its mass inside $[a,b]$.

Now we expand the functions $f(y)$ and $v(y)$ using the Fourier-cosine basis such that

$$P_1 = \int_a^b v(y)f(y)dy = \frac{b-a}{2}{\sum_{k=0}^{\infty}}' A_k \cdot V_k \tag{10}$$

$\sum'$ indicates that the first term in the summation has a weight of one half. A_k are the Fourier-cosine series expansion coefficients for the density function $f(y)$ and V_k are the Fourier-cosine series expansion coefficients for $v(y)$ over the same interval $[a,b] \in \mathbb{R}$:

$$\begin{aligned} f(y) &= {\sum_{k=0}^{\infty}}' A_k \cos\left(k\pi\frac{y-a}{b-a}\right), \\ v(y) &= {\sum_{k=0}^{\infty}}' V_k \cos\left(k\pi\frac{y-a}{b-a}\right). \end{aligned}$$

Using orthogonality, A_k and V_k take the form

$$A_k = \frac{2}{b-a}\int_a^b f(y)\cos\left(k\pi\frac{y-a}{b-a}\right)dy = \frac{2}{b-a}\mathrm{Re}\left\{\int_a^b f(y)e^{ik\pi\left(\frac{y-a}{b-a}\right)}dy\right\}; \tag{11}$$

$$V_k = \frac{2}{b-a}\int_a^b v(y)\cos\left(k\pi\frac{y-a}{b-a}\right)dy. \tag{12}$$

For a general setting, Fang and Oosterlee (2008) recommend using $[a,b]$ covering $\pm$ 10 times the standard deviation of the underlying random variable centered on the mean of the random variable, to reduce the approximation error between P and P_1.

2. *Finite Frequency Approximation*: When N is sufficiently large, we can approximate P_1 with the P_2 below by discarding the tail terms,

$$P_2 = \frac{b-a}{2}{\sum_{k=0}^{N-1}}' A_k \cdot V_k. \tag{13}$$

The convergence of the sequence depends on the smoothness of the density function. Fang and Oosterlee (2008) state that if the function is smooth, continuous, and without singularity, exponential convergence is attained – otherwise, an algebraic index of convergence is attained.

In the general application of the COS method, it is important to determine the optimal size of the truncated region $[a, b]$. One cannot choose an arbitrage large domain $[a, b]$ to minimize the first level error $|P - P_1|$. Since the larger the domain, the more number of COS expansion terms is needed to get a predetermined second level error $|P_1 - P_2|$. Hence it need more resources to calculate the coefficients and the summation.

3. *Characteristic Function Approximation*: A_k can be written in an equivalent form using the partial characteristic function of $f(x)$.

$$A_k = \frac{2}{b-a} \mathrm{Re}\left\{ \phi^{ab}\left(\frac{k\pi}{b-a}\right) e^{\frac{-ik\pi a}{b-a}} \right\}, \tag{14}$$

where

$$\phi^{ab}(u) = \int_a^b e^{iuy} f(y) dy \tag{15}$$

is close to the characteristic function but the domain is limited to $[a, b]$. This final approximation replaces $\phi^{ab}(u)$ with the true characteristic function,

$$\phi(u) := \int_{\mathbb{R}} e^{iuy} f(y) dy.$$

This replacement results in the approximation of the Fourier series coefficients A_k

$$\tilde{A}_k \approx \frac{2}{b-a} \mathrm{Re}\left\{ \phi\left(\frac{k\pi}{b-a}\right) e^{\frac{-ik\pi a}{b-a}} \right\}.$$

The approximate payoff function is then given by

$$P_3 = \frac{b-a}{2} \sum_{k=0}^{N-1}{}' \tilde{A}_k \cdot V_k,$$

and the error $|P_2 - P_3|$ depends on the size of domain $[a, b]$.

Using each of the above approximations and simplifications, the COS method payoff takes the form

$$P_3 = \sum_{k=0}^{N-1}{}' \mathrm{Re}\left\{ \phi\left(\frac{k\pi}{b-a}\right) e^{\frac{-ik\pi a}{b-a}} \right\} \cdot V_k. \tag{16}$$

Once the Fourier series of the payoff function has been determined, the computation of the payoff for any model with a defined characteristic function is easily computed with Equation (16).

The COS method features an important "separation" property: the payoff information (EIA structural design parameters) is contained in the Fourier coefficients V_k; and the distribution information is contained in the characteristic function $\phi(u)$.

3.2 The First Level COS expansion

The present value of the annuity contract is given by an integral of the payoff function with the PDF of the capped return variable D – see Section 2. Applying the COS method to approximate its value results in the following expression

$$\begin{aligned} PV &= e^{-\hat{r}T} \int v(y) f_D(y) dy \\ &= e^{-\hat{r}T} \int K \max(1+g, 1+y) f_D(y) dy \\ &= e^{-\hat{r}T} \sum_{k=0}^{N-1}{}' \mathrm{Re}\left\{ \phi_D\left(\frac{k\pi}{b-a}\right) e^{\frac{-ik\pi a}{b-a}} \right\} \cdot V_k. \end{aligned} \quad (17)$$

The payoff function $v(y) = K \max(1+g, 1+y)$ and the Fourier-cosine series coefficients V_k are given by

$$V_k = \frac{2}{b-a} \int_a^b K \max(1+g, 1+y) \cos\left(k\pi \frac{y-a}{b-a}\right) dy. \quad (18)$$

V_k can be valued by elementary integrations. In order to simplify the form of V_k, first introduce two functions

$$\chi_k(c,d) := \int_c^d y \cos\left(k\pi \frac{y-a}{b-a}\right) dy \qquad \text{and} \qquad \psi_k(c,d) := \int_c^d \cos\left(k\pi \frac{y-a}{b-a}\right) dy. \quad (19)$$

These elementary integrals have the following expressions

$$\chi_k(c,d) = \begin{cases} \begin{array}{l} \left[\sin\left(k\pi\frac{d-a}{b-a}\right)\frac{k\pi d}{b-a} - \sin\left(k\pi\frac{c-a}{b-a}\right)\frac{k\pi c}{b-a} \right. \\ \left. + \cos\left(k\pi\frac{d-a}{b-a}\right) - \cos\left(k\pi\frac{c-a}{b-a}\right)\right]\left(\frac{b-a}{k\pi}\right)^2 \end{array}, & k \neq 0; \\ \frac{1}{2}(d^2 - c^2), & k = 0. \end{cases} \quad (20)$$

and

$$\psi_k(c,d) = \begin{cases} \left(\sin\left(k\pi\frac{d-a}{b-a}\right) - \sin\left(k\pi\frac{c-a}{b-a}\right)\right)\frac{b-a}{k\pi}, & k \neq 0; \\ d - c, & k = 0. \end{cases} \quad (21)$$

V_k is thus expressed in terms of χ_k and ψ_k as

$$V_k = \frac{2K}{b-a}\left(\chi_k(g,b) + \psi_k(a,b) + g\psi_k(a,g)\right). \quad (22)$$

assuming $a < g < b$.

This section demonstrated how to compute the coefficients $V(k)$ in the payoff Equation (17). In the following section, we will show how the characteristic function of the capped return variable D is computed. Again, we directly use the COS method to construct the characteristic function.

3.3 Second Application of the COS Method

First, by introducing a return variable $C_j = \min(c, R_j)$, the capped return variable D can be rewritten as

$$D = \sum_{j=1}^{n} C_j.$$

Since the $\{C_j\}_{j=1,\dots,n}$ are independent and identically distributed random variables, the characteristic function of D is simply a product of the characteristic functions of C_j

$$\phi_D(u) = \phi_C^n(u).$$

Here, we drop the subscript j to reflect the fact that $\phi_{C_j}(u)$ are identical. In our second application, we apply the COS method to construct the characteristic function ϕ_C. Note that the characteristic function is also defined in an integral of the form

$$\begin{aligned} \phi_C(u) := \mathbb{E}[e^{iuC}] &= \mathbb{E}\left[e^{iu\min(c,R)}\right] \\ &= \mathbb{E}\left[e^{iu\min\left(c,e^X-1\right)}\right] \\ &= \int_{\mathbb{R}} e^{iu\min(c,e^y-1)} f_X(y)dy, \end{aligned} \tag{23}$$

where X_j is the log-return $X_j = \log\left(S(t_j)/S(t_{j-1})\right)$. The holding period return R_j is related to the log-return by

$$R_j = e^{X_j} - 1.$$

This integral form invites a second application of the COS method. In particular, approximating the characteristic function with the COS method, we find that

$$\tilde{\phi}_C(u) := \sum_{k=0}^{\tilde{N}-1}{}' \mathrm{Re}\left\{\phi_X\left(\frac{k\pi}{\tilde{b}-\tilde{a}}\right) e^{\frac{-ik\pi\tilde{a}}{\tilde{b}-\tilde{a}}}\right\} \cdot \tilde{V}_k(u) \tag{24}$$

where

$$\begin{aligned} \tilde{V}_k(u) &= \frac{2}{\tilde{b}-\tilde{a}} \int_{\tilde{a}}^{\tilde{b}} e^{iu\min(c,e^y-1)} \cos\left(k\pi\frac{y-\tilde{a}}{\tilde{b}-\tilde{a}}\right) dy \\ &= \frac{2}{\tilde{b}-\tilde{a}} \left[\psi_k\left(\log(1+c),\tilde{b}\right) e^{iuc} + e^{-iu} \int_{\tilde{a}}^{\log(1+c)} e^{iue^y} \cos\left(k\pi\frac{y-\tilde{a}}{\tilde{b}-\tilde{a}}\right) dy\right], \end{aligned} \tag{25}$$

and ϕ_X is the characteristic function of the underlying asset return model. Generally speaking, there need not be a correspondence between the ranges $[a, b]$ and $[\tilde{a}, \tilde{b}]$ or the number of terms in the expansions N and $\tilde{N}$ in the two separate applications of the COS method.

For convenience, we define a function

$$\tilde{\gamma}_k(c,d,u) = \int_c^d e^{iue^y} \cos\left(k\pi \frac{y-\tilde{a}}{\tilde{b}-\tilde{a}}\right) dy,$$

so that

$$\tilde{V}_k(u) = \frac{2}{\tilde{b}-\tilde{a}} \left[\tilde{\psi}_k\left(\log(1+c), \tilde{b}\right) e^{iuc} + e^{-iu}\tilde{\gamma}_k\left(\tilde{a}, \log\left(1+c\right), u\right)\right]. \tag{26}$$

Unfortunately, $\tilde{\gamma}_k(c,d,u)$ does not have a closed-form expression. As a result, $\tilde{\phi}_C(u)$ takes only discrete input values $u \in \left\{\frac{k\pi}{b-a} | k = 0, 1, \ldots, N-1\right\}$. A matrix of $N \times \tilde{N}$ must be computed for this valuation. This matrix, $U(k,k')$, is defined as

$$U(k,k') = \tilde{V}_{k'}\left(\frac{k\pi}{b-a}\right), \tag{27}$$

for $k = 0, 1, \ldots, N-1$ and $k' = 0, 1, \ldots, \tilde{N}-1$.

Summarizing all the steps above, the present value of the annuity contract is

$$PV = e^{-\hat{r}T} {\sum_{k=0}^{N-1}}' \text{Re}\left\{\tilde{\phi}_C^n\left(\frac{k\pi}{b-a}\right) e^{\frac{-ik\pi a}{b-a}}\right\} \cdot V_k. \tag{28}$$

V_k is derived in Equation (22) and the characteristic function $\tilde{\phi}_C(u)$ is defined in Equation (24). To further value $\tilde{\phi}_C(u)$, we need to compute $\tilde{V}_k(u)$ via Equation (26) and using corresponding characteristic function ϕ_X of logarithmic return of index.

4 Application to Lévy Processes

4.1 Alternative One Level COS Solution for APP

The two-level COS application is generally applicable for APP and MPP contracts. However, due to the discontinuity of the underlying PDF of the capped return variable, D, on the upper boundary, the COS method converges algebraically and usually requires a large number of basis.[3] So instead of using the two level COS method, in APP we recommend to model the return variable X directly using COS method.

[3] This discontinuity of the PDF function on the upper boundary also exists for the MPP contracts, however, it causes little trouble in the real world compared to the APP contracts. In MPP the probability that D reaches its upper limit, $12c$, is tiny. When $D = 12c$, it means the EIAs obtain the cap return every month. This probability is around 0.8×10^{-5} using the parameters in our simulations (see Section 5.1). While in APP, the probability of D reaches its upper limit c is relatively large.

Recall the following relationship:

$$D = \min(c, R) = \min(c, e^X - 1).$$

The annuity's value is written in terms of the characteristic function of the return variable X using the COS method

$$\begin{aligned} PV &= e^{-\hat{r}T} \int K \max(1+g, 1+y) f_D(y) dy \\ &= e^{-\hat{r}T} \int K \max(1+g, 1+\min(c, y)) f_R(y) dy \\ &= e^{-\hat{r}T} \int K \max(1+g, 1+\min(c, e^y - 1)) f_X(y) dy \\ &= e^{-\hat{r}T} \sum_{k=0}^{N-1}{}' \mathrm{Re}\left\{ \phi_X\left(\frac{k\pi}{b-a}\right) e^{\frac{-ik\pi a}{b-a}} \right\} \cdot \hat{V}_k. \end{aligned} \tag{29}$$

Here we use the fact the payoff function $\hat{v}(y) = K \max(1+g, 1+\min(c, e^y - 1))$. Following the general rule in the COS method, we have

$$\begin{aligned} \hat{V}_k &= \frac{2}{b-a} \int_a^b \hat{v}(y) \cos\left(k\pi \frac{y-a}{b-a}\right) dy \\ &= \frac{2}{b-a} \int_a^b K \max(1+g, 1+\min(c, e^y - 1)) \cos\left(k\pi \frac{y-a}{b-a}\right) dy \\ &= \frac{2K}{b-a} (\psi_k(a, b) + \psi_k(c, b) + \psi_k(a, g) - \psi_k(\log(g+1), \log(c+1)) \\ &\quad + \varphi_k(\log(g+1), \log(c+1))), \end{aligned} \tag{30}$$

where we introduce a new function $\varphi_k(c, d)$ with closed form derived directly via elementrary calculus again:

$$\begin{aligned} \varphi_k(c, d) &:= \int_c^d e^y \cos\left(k\pi \frac{y-a}{b-a}\right) dy \\ &= \frac{1}{1 + \left(\frac{k\pi}{b-a}\right)^2} \left[\cos\left(k\pi \frac{d-a}{b-a}\right) e^d - \cos\left(k\pi \frac{c-a}{b-a}\right) e^c \right. \\ &\quad \left. + \frac{k\pi}{b-a} \sin\left(k\pi \frac{d-a}{b-a}\right) e^d - \frac{k\pi}{b-a} \sin\left(k\pi \frac{c-a}{b-a}\right) e^c \right]. \end{aligned} \tag{31}$$

4.2 Alternative $\phi_C(t)$ Formulation

Instead of using the (second level) COS method to construct the characteristic function D, there are alternative ways to compute the characteristic function. Bernard and Li (2012) propose using the probability distribution of R,

$$\phi_C(u) = \mathbb{E}[e^{iuC}] = e^{-iu}\left(1 + iu\int_0^{1+c} e^{iux}Q(R \geq x-1)dx\right). \tag{32}$$

The characteristic function $\phi_C(t)$ can be rearranged in terms of X.

$$\begin{aligned}\phi_C(u) &= e^{-iu}\left(1 + iu\int_0^{1+c} e^{iux}Q(X \geq \log(x))dx\right) \\ &= e^{-iu}\left(1 + iu\int_0^{1+c} e^{iux}(1 - F_X(\log(x))dx\right).\end{aligned} \tag{33}$$

The general form of the cumulative distribution function, $F_X(x)$, is (Bernard and Li, 2012).

$$F_X(x) = \frac{e^{ax}}{2\pi}\int e^{iux}\frac{\phi_X(ia-u)}{a+iu}du. \tag{34}$$

The drawback of deriving the characteristic function $\phi_C(t)$ using Equation (33) and Equation (34) is the double-integral calculation therein. For the Black-Scholes model, the characteristic function in Equation (33) could be simplified and provides an accurate valuation of the function. For other general Lévy process based models, evaluation of the double-integral is not practical. In Section 5.1, we use this alternative approach in the Black-Scholes model to test the rate of convergence and perform error analysis for the two levels of the COS method.

4.3 Greeks

The separation property of the COS method means that all of the dynamic information about the underlying price process is contained within the characteristic function. As a result, any sensitivity to market conditions can be computed as a derivative of the characteristic function. For example, in the Black-Scholes setting, the sensitivity to volatility (vega) is given by

$$\frac{\partial PV}{\partial\sigma} = e^{-\hat{r}T}{\sum_{k=0}^{N-1}}'\mathrm{Re}\left\{n\tilde{\phi}_C^{n-1}\left(\frac{k\pi}{b-a}\right)\frac{\partial\tilde{\phi}_C}{\partial\sigma}\left(\frac{k\pi}{b-a}\right)e^{\frac{-ik\pi}{b-a}}\right\}\cdot V_k. \tag{35}$$

where V_k is independent of σ since V_k encodes only information about the EIA payoff structure. Further, since $\tilde{V}_k$ is also independent of σ, we can evaluate the partial derivative of the characteristic function as

$$\frac{\partial\tilde{\phi}_{C_j}}{\partial\sigma}(u) = {\sum_{k=0}^{\tilde{N}-1}}'\mathrm{Re}\left\{\frac{\partial\phi_X}{\partial\sigma}\left(\frac{k\pi}{b-a}\right)e^{\frac{-ik\pi}{b-a}}\right\}\cdot\tilde{V}_k(u). \tag{36}$$

This separation property reduces the complexity of determining sensitivities to linear combinations of partial derivatives of the characteristic function.

4.4 Black-Scholes Model

We will illustrate how to apply the method described above within several Lévy based models. The first example is the Black-Scholes (BS) model, under which, the index level follows a geometric Brownian process

$$\frac{dS_t}{S_t} = (\mu - q)dt + \sigma dW_t, \tag{37}$$

where W_t is a Brownian process. The monthly return R_j follows a shifted lognormal distribution $R_j = e^{X_j} - 1$ where the monthly log-return X_j is a normally distributed random variable. Under the risk-neutral measure $\mathbb{Q}$, the monthly return (over time interval Δ) is given by

$$X \sim \mathcal{N}((r - q - \sigma^2/2)\Delta, \sigma^2\Delta). \tag{38}$$

Let $m_X = (r - q - \sigma^2/2)\Delta$ and $\sigma_X = \sigma\sqrt{\Delta}$ denote the mean and standard deviation of the random variable X. The characteristic function for the Black-Scholes model is then given by

$$\phi_X(u) = e^{itm_X - \frac{1}{2}u^2\sigma_X^2}. \tag{39}$$

and

$$\frac{\partial\phi_X(u)}{\partial\sigma} = (-iu\sigma\Delta - u^2\sigma\Delta)e^{itm_X - \frac{1}{2}u^2\sigma_X^2}. \tag{40}$$

Bernard and Li (2012) have directly computed $\phi_C(u)$ using the alternative method in Section 4.2

$$\phi_C(u) = \mathbb{E}\left[e^{iuC}\right] = e^{-iu}\left(1 + iu\int_0^{1+c} e^{iux} N\left(\frac{m_X - \log(x)}{\sigma_X}\right) dx\right). \tag{41}$$

Taking the partial derivative with respect to σ reveals an expression for vega in the Black-Scholes model given in Equation (4.6) of Bernard and Li (2012).

4.5 CGMY Model

The CGMY process, introduced by Carr et al. (2002), generalizes the Black-Scholes model to include pathwise discontinuities. The CGMY Lévy density is given by

$$k(x) = \begin{cases} C\frac{e^{-G|x|}}{|x|^{1+Y}}, & x < 0; \\ C\frac{e^{-M|x|}}{|x|^{1+Y}}, & x > 0. \end{cases} \tag{42}$$

The extended CGMY model includes an orthogonal diffusion component and has a characteristic function given by

$$\phi_X(u) = \exp\left(iu\left[(r - q + \omega)\Delta\right]\right) \times \phi_{CGMY}(u, \Delta) \tag{43}$$

where the CGMY characteristic function takes the form

$$\begin{aligned}\phi_{CGMY}(u,\Delta) &= \exp\left\{\Delta\int_{\mathbb{R}}(e^{iux}-1)k(x)dx\right\}\\ &= \exp\left\{\Delta C\Gamma(-Y)\left[(M-iu)^Y-M^Y+(G+iu)^Y-G^Y\right]\right\}\end{aligned} \tag{44}$$

and the convexity correction is

$$\omega = -\frac{1}{\Delta}\ln\phi_{CGMY}(-i,\Delta). \tag{45}$$

The variance gamma (VG) model is a special case of the CGMY model with

$$C=\frac{1}{\nu},\quad G=\frac{2}{\sqrt{\theta^2\nu^2+2\sigma^2\nu}+\theta\nu},\quad M=\frac{2}{\sqrt{\theta^2\nu^2+2\sigma^2\nu}-\theta\nu},\quad \text{and}\quad Y=0. \tag{46}$$

To be explicit, the VG model has the characteristic function

$$\phi_{VG}(u,\Delta)=\left(1-i\theta\nu u+\frac{1}{2}\sigma^2\nu u^2\right)^{-\Delta/\nu}. \tag{47}$$

For more information about the use of Lévy processes in finance, see Schoutons (2003).

5 Numerical Examples

In this section, we illustrate our methodology with both APP and MPP crediting formulas. We pay special attention to convergence speed and error analysis when setting parameters of the COS method. Although we present applications to the one-year APP and MPP, generalization to multiple years is trivial.

5.1 Black-Scholes Example

5.1.1 Annual Point-to-Point

In APP contracts, the return variables X, R and D are all annual return variables. The rate of convergence of the second level COS method is dependent on the smoothness of the density function of the annual return X and exponential convergence is typically achieved. We found numerically that the error is well-controlled for $\tilde{N} \leq 100$ number of terms. However, the first level COS method uses the density function of capped return variable $D = \min(c, e^X - 1)$ which only converges algebraically. In our test, as many as 500 terms may be required to achieve similar accuracy at the second level of the COS method. In practice, we recommend using the alternative one-level COS approach in Section 4.1 to handle the APP type contracts. Moreover, there is no need to perform a pre-calculation matrix in the one-level COS method.

The parameters used for the Black-Scholes model in our example are as follows: the risk free rate $r = 3\%$, the dividend yield $q = 1\%$, the volatility $\sigma = 20\%$ and the insurer rate $\hat{r} = 5\%$. For the EIA contract, we set minimum guaranteed return for one year $g = 3\%$, with an annual cap $c = 8\%$. The initial EIA investment is assumed to be $K = \$1,000$. The choice of parameters used in the COS method $[a, b]$ and N warrants further discussion.

Fourier expansion relies on the annual return X, which follows a normal distribution with mean $r - q$ and volatility σ, therefore, according to suggestions by Fang and Oosterlee (2008) the truncated range $[a, b]$ should be set to $[r - q - 10\sigma, r - q + 10\sigma]$, or roughly $[-10\sigma, 10\sigma]$. Using the default $\sigma = 20\%$, we eventually set the truncated range $[a, b] = [-2, 2]$.

To compute an accurate reference value for comparison, we used a large number of terms ($N = 200$). We find decaying error as N increases, and the calculation error as a function of N is presented in Figure 1.

Figure 1: Annual point-to-point (APP) equity-indexed annuity estimation error within the Black-Scholes model using the COS method.

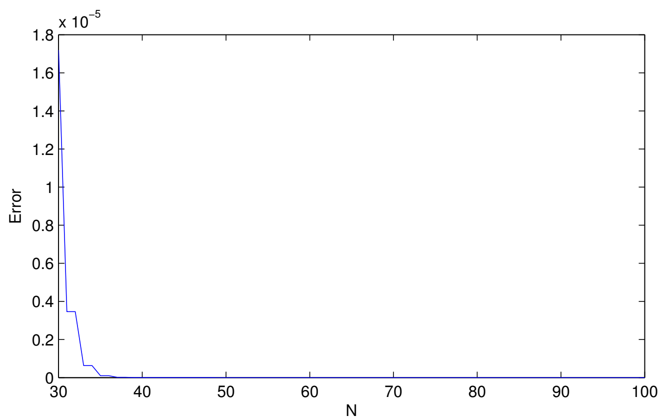

Using roughly $N = 30$ we achieve an accuracy on the scale of 10^{-5}. The error decreases further with increasing N and for $N \geq 50$ the error is at the 10^{-8} level.

In Figure 2, we illustrate the dependence of the EIA value and vega on the volatility σ of the underlying index in the Black-Scholes model. The range of volatility used for testing purposes is 10% to 40%. For the COS method, we varied the range $[a, b]$ as a function of volatility levels $[-10\sigma, 10\sigma]$. As a comparison, we also computed the EIA value and vega using Monte Carlo simulations with 10,000 replications. Since vega represents changes of the EIA value with respect to changes in the volatility parameter σ. To obtain a better accuracy in our simulation of vega, we fixed a common random seed in the simulations. For a given volatility σ, vega is computed as the changes in the annuity value given an infinitesimal change in the volatility $\sigma \pm \kappa\sigma$, where κ is a small value.

Figure 2: Annual point-to-point (APP) equity-indexed annuity value and vega estimation within the Black-Scholes model using the COS method.

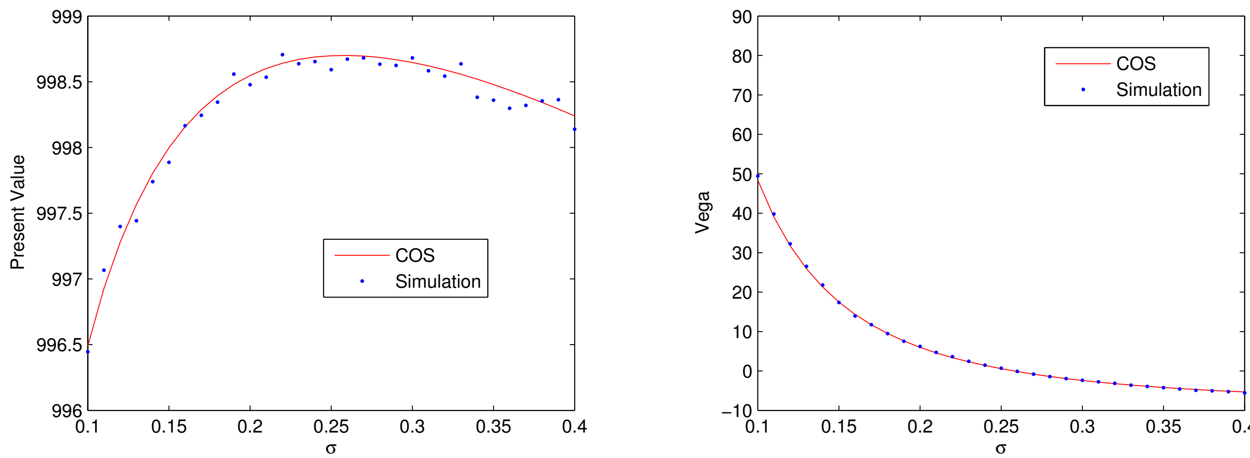

(a) Value estimation error (b) Vega estimation error

Although the behavior of the two numerical approximations agrees quite well, the results of the Monte Carlo simulations contain much more noise than the smooth results of the COS method. This is despite the fact that 10,000 simulations are used for the Monte Carlo results and only 50 terms are used for the COS method.

5.1.2 Monthly Point-to-Point

We use the two-level COS method in the Black-Scholes model to value a MPP with $n = 12$ for 12 observation periods and a monthly cap of $c = 2\%$. Since X_j is the monthly return variable with a normal distribution, we used the range $\left[\tilde{a}, \tilde{b}\right] = [-10\sigma/\sqrt{n}, 10\sigma/\sqrt{n}]$. In preparation for the volatility dependence illustration where $\sigma = 10\% - 40\%$, we fixed the range $[\tilde{a}, \tilde{b}] = [-1, 1]$ calculated by using the maximum volatility 40%.

We find that 100 for both N and $\tilde{N}$ provide good accuracy. Therefore, the two-level COS method relies on the calculation of a 100×100 matrix U (Equation (27)) that depends on the monthly cap, c, and on the interval, $[a, b]$.[4]

Since the capped return $D = \sum_{j=1}^{12} C_j = \sum_{j=1}^{12} \min(c, e^{X_j} - 1)$ has a smaller volatility than the annual return, we use $a = -10\sigma = -4$ and $b = nc = 0.24$ for the first level of the COS method. (Note that as we point out before, D's domain is $[-n, nc]$.) To show the convergence rate as a function of N, we use the Black-Scholes characteristic function in Equation (41) instead of the

[4] Calculation of these matrix elements takes approximately 90 seconds on an i7 machine with 8G of RAM. Further gains in efficiency can be realized by using parallel computing tools.

second application of COS method and vary the number of terms N. Our results are presented in Figure 3(a). The error is no longer appreciable when $N \geq 70$.

To show the convergence on the second level of the COS method, we fix $N = 100$ and vary the number $\tilde{N}$. The error is estimated by comparing the value obtained using the two-level COS method with the BS characteristic function of Bernard et al. (2011). The results are illustrated in Figure 3(b).

Figure 3: Example of numerical convergence for a monthly point-to-point (MPP) equity-indexed annuity within the Black-Scholes model using the COS method.

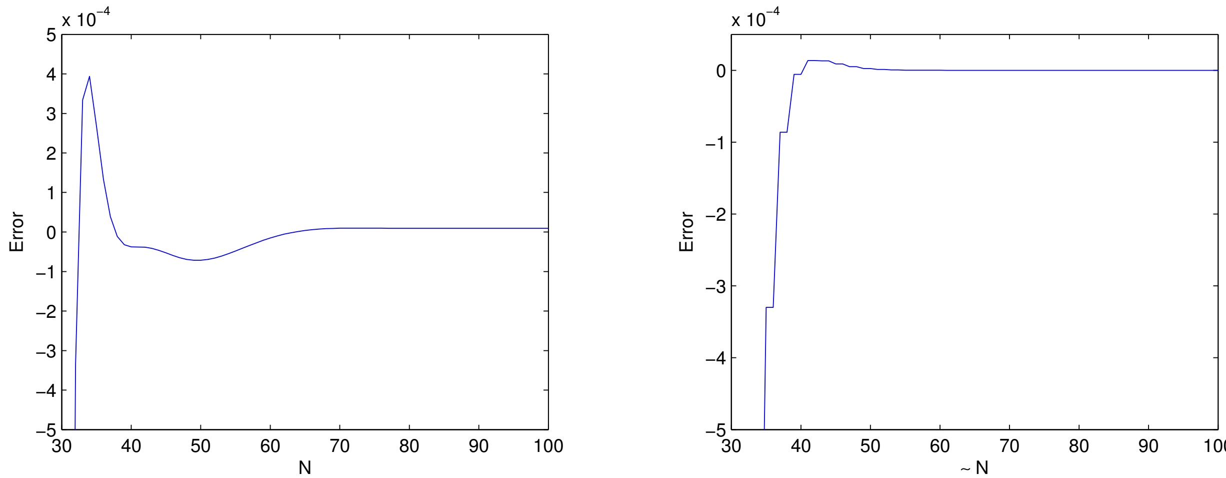

(a) Error as a function of N

(b) Error as a function of $\tilde{N}$

In Figure 4, we illustrate the dependence of the EIA value and vega on the volatility of the underlying index in the Black-Scholes model. As in Figure 2, we also computed the EIA value and vega using Monte Carlo simulations with 10,000 replications.

Figure 4: Monthly point-to-point (MPP) equity-indexed annuity value and vega estimation within the Black-Scholes model using the COS method.

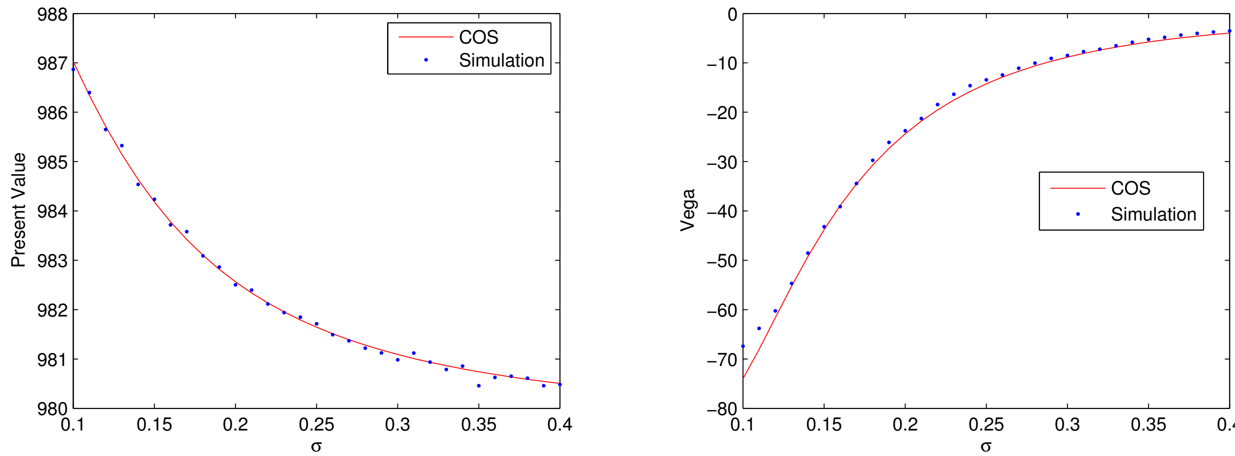

(a) Value estimation error (b) Vega estimation error

We once again see the agreement between the behavior of the two numerical approximations. Monte Carlo simulations with a similar level of smoothness for either value of the EIA require significantly more computational resources than the two-level COS method described here.

5.2 CGMY Example

5.2.1 Annual Point-to-Point

We use model parameters $C = 25$, $G = 95$, $M = 95$, and $Y = 0.25$ for the CGMY model. The parameter set is chosen to be close to the parameter set calibrated by the S&P 500 index in found in Carr et al. (2002). To determine the region $[a, b]$ to use for the COS method, we estimate the standard deviation of returns resulting from this price process. We use the COS method to estimate the standard deviation by numerically computing both $\mathbb{E}(X^2)$ and $\mathbb{E}(X)$ and the fact that $var(X) = \mathbb{E}(X^2) - \mathbb{E}(X)^2$. Using the above CGMY parameters, we find that the standard deviation of the distribution is approximately 12.61% and as a result use $[a, b] = [-10\sigma, 10\sigma] \approx [-1.26, 1.26]$.

In Figure 5, we show the convergence of the COS method to the product value of \$997.4387 as a function of the number of terms in the series.

Figure 5: APP Error.

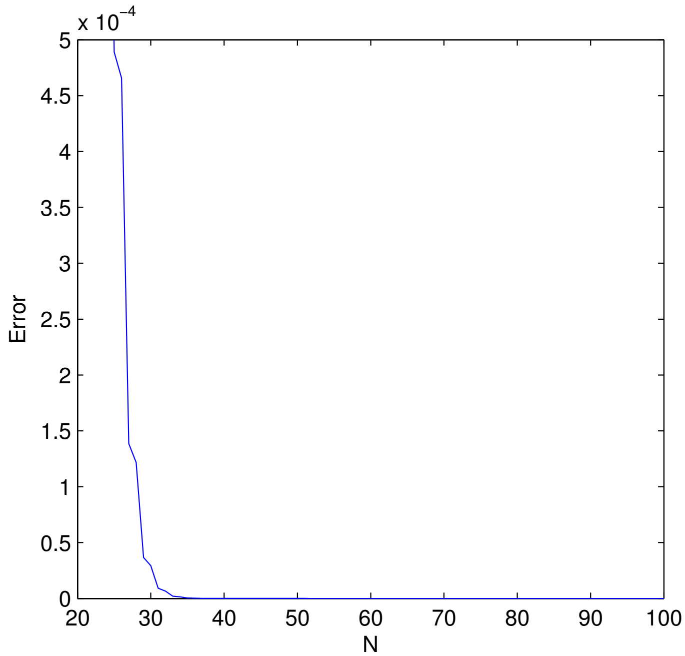

Our results indicate that a relatively small number of terms is required – $N \geq 50$ – to reach an adequate level of precision.

5.2.2 Monthly Point-to-Point

For a MPP product with a 2% cap, the product value is \$985.4757. For this case, we choose $[\tilde{a}, \tilde{b}] = [-1.26/\sqrt{12},\ 1.26/\sqrt{12}] = [-0.36,\ 0.36]$ and $[a, b] = [-1.26,\ 0.24]$. In Figure 6, we show the convergence of the two-level COS method for different number of terms.

Figure 6: Example of numerical convergence for a monthly point-to-point (MPP) equity-indexed annuity within the CGMY model using the COS method.

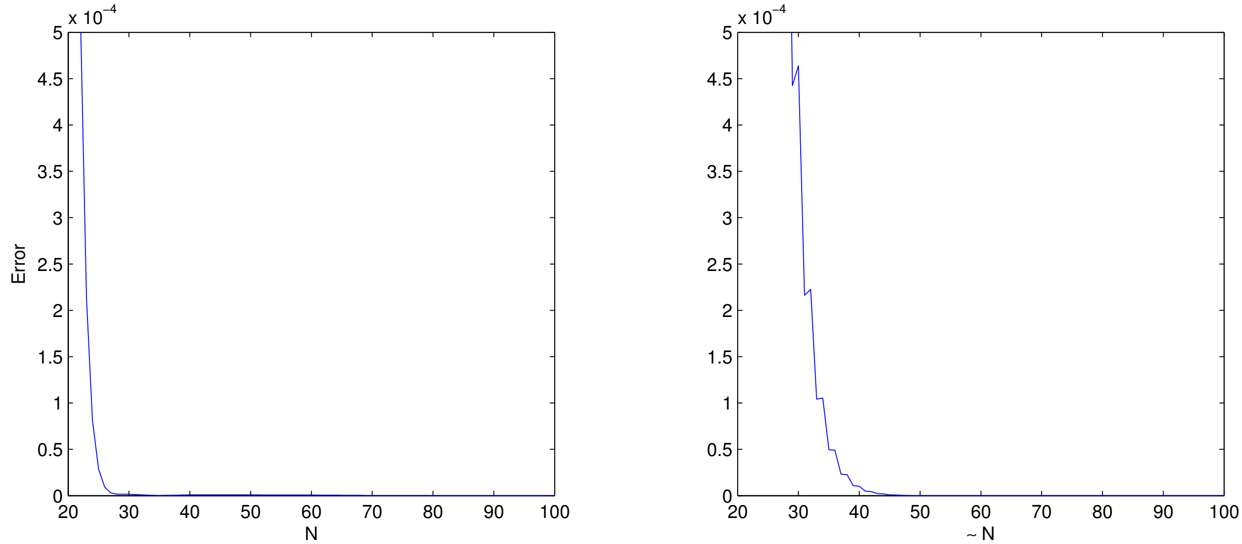

(a) Error as a function of N (b) Error as a function of $\tilde{N}$

For both levels, the COS uses roughly 50 steps to converge to the desired accuracy level.

As we have discussed before, the truncation range $[a, b]$ should be set according to the size of volatility. However, we observe that a larger size $[a, b]$ typically results in a slower rate of convergence. Though the there is a high rate of convergence in our examples, this number could rise significantly if a larger truncation region is required.

6 Conclusions

In this paper, we proposed an algorithm that efficiently values point-to-point EIAs under general Lévy-process based index returns by extending the COS method of Fang and Oosterlee (2008). We expressed the value of an EIA contract as a series of characteristic function evaluations. We presented several Lévy process examples, including the Black-Scholes model and the CGMY model, to illustrate the effectiveness of the algorithm. We also showed how the algorithm can be used to efficiently compute EIA market sensitivities, facilitating hedging of these instruments. Finally, we presented a numerical analysis of the convergence and efficiency of the numerical valuation approach suggested here.

Although we focused on the point-to-point design and gave particular examples of price processes, our methodology is much more general. It can be applied to nearly any path-dependent option embedded in an EIA and can be based on any price process that has a closed-form characteristic function. Future research directions include the study of alternative bases for the expansion as well as the application of our methodology to other annuity payoff structures.

References

L. Ballotta. Efficient pricing of ratchet equity-index annuities in a variance-gamma economy. *North American Actuarial Journal*, 14(3):355–368, 2010.

C. Bernard and P. Boyle. A natural hedge for equity indexed annuities. *Annals of Actuarial Science*, 5(2):211–230, 2011.

C. Bernard and W. Li. Pricing and hedging of cliquet options and locally capped contracts. *SIAM Journal on Financial Mathematics*, 4(1):353–371, 2012.

C. Bernard, P. Boyle, and W. Gornall. Locally-capped investment products and the retail investor. *Journal of Derivatives*, 18(4):72–88, 2011.

P. Boyle and W. Tian. The design of equity-indexed annuities. *Insurance: Mathematics and Economics*, 43(3):303–315, 2008.

P. Carr, H. Geman, D. Madan, and M. Yor. The fine structure of asset returns: An empirical investigation. *Journal of Business*, 75(2):305–332, 2002.

F. Fang and C. Oosterlee. A Fourier-based valuation method for bermudan and barrier options under Heston's model. *SIAM Journal of Financial Mathematics*, 2(1):439–463, 2011.

F. Fang and C. W. Oosterlee. A novel pricing method for european options based on fourier-cosine series expansions. *SIAM Journal on Scientific Computing*, 31(2):826–848, 2008.

F. Fang and C. W. Oosterlee. Pricing early-exercise and discrete barrier options by fourier-cosine series expansions. *Numerische Mathematik*, 114:27–62, 2009.

P. Gaillardetz and S. Lin. Valuation of equity-linked insurance and annuity products with binomial models. *North American Actuarial Journal*, 10(4):117–144, 2006.

S. Jaimungal. Pricing and hedging equity indexed annuities with variance-gamma deviates. 2004. Working Paper.

S. Jaimungal and V. Young. Pricing equity-linked pure endowments with risky assets that follow Lévy processes. *Insurance: Mathematics and Economics*, 36(3):329–346, 2005.

M. Kijima and T. Wong. Pricing of ratchet equity-indexed annuities under stochastic interest rates. *Insurance: Mathematics and Economics*, 41(3):317–338, 2007.

H. Lee. Pricing equity-indexed annuities with path-dependent options. *Insurance: Mathematics and Economics*, 33(3):677–690, 2003.

X. Lin and K. Tan. Valuation of equity-indexed annuities under stochastic interest rates. *North American Actuarial Journal*, 7(3):72–91, 2003.

D. Madan, P. Carr, and E. Chang. The variance gamma process and option pricing. *European Finance Review*, 2:79–105, 1998.

D. B. Madan and W. Shoutens. Simple processes and the pricing and hedging of cliquets. *Mathematical Finance*, 23(1):198–216, 2013.

W. Schoutons. *Lévy Processes in Finance*. Wiley, 2003.

S. Tiong. Valuing equity-indexed annuities. *North American Actuarial Journal*, 4(4):149–170, 2010.

P. Wilmott. Cliquet options and volatility models. *Wilmott Magazine*, pages 379–390, 2002.

H. Windcliff, P. Forsyth, and F. Vetzal. Numerical methods and volatility models for valuing cliquet options. *Applied Mathematical Finance*, 13(4):353–386, 2006.

F. L. Yuen and H. Yang. Pricing Asian options and equity-indexed annuities with regime switching by the trinomial tree method. *North American Actuarial Journal*, 14(2):256–277, 2010.

B. Zhang and C. W. Oosterlee. Efficient pricing of European-style Asian options under exponetial Lévy processes based on Fourier cosine expansions. *SIAM Journal of Financial Mathematics*, 4 (1):399–426, 2013.